

**Investigation of the Heterogeneous Ice Nucleation Potential of Sea Spray Aerosol**

by

Lilian A. Dove

Submitted to the Department of Earth, Atmospheric and Planetary Sciences

in Partial Fulfillment of the Requirements for the Degree of

Bachelor of Science in Earth, Atmospheric and Planetary Sciences

at the Massachusetts Institute of Technology

May 18, 2018 [June 2018]

Copyright 2018 Lilian A. Dove. All rights reserved.

The author hereby grants to MIT permission to reproduce and to distribute publicly paper and electronic copies of this thesis document in whole or in part in any medium now known or hereafter created.

Author \_\_\_\_\_ **Signature redacted**

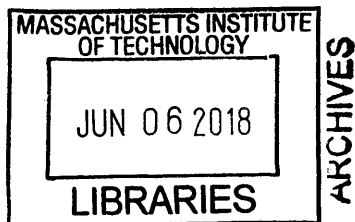
Department of Earth, Atmospheric and Planetary Sciences  
May 18, 2018

Certified by \_\_\_\_\_ **Signature redacted**

Daniel J. Cziczo  
Thesis Supervisor

Accepted by \_\_\_\_\_ **Signature redacted**

Richard P. Binzel  
Chair, Committee on Undergraduate Program



# Investigation of the Heterogeneous Ice Nucleation Potential of Sea Spray Aerosol

Lilian A. Dove

May 15, 2018

## **Abstract**

Bubble bursting at the ocean surface generates smaller film-burst particles and larger jet drop particles that differ in composition. The chemical composition of sea spray aerosols is an important parameter for the evaluation of their impact on the global climate system. This study investigates the role of particle chemistry on the heterogeneous ice nucleation potential of laboratory-generated sea spray aerosols. Cultures of *Prochlorococcus*, a highly abundant marine phytoplankton species, were used as a model source of organic sea spray aerosols. Results show that smaller particles generated from the lysed *Prochlorococcus* cultures were organically enriched and effectively activated as ice nucleating particles at warmer temperatures and lower supersaturations than larger particles. The role of chemical composition in the activation of the particles was studied by measuring the nucleation abilities of single component organic molecules that mimic proteins, lipids, and carbohydrates in *Prochlorococcus*. Amylopectin, agarose, and aspartic acid exhibited nucleation behaviors similar to particles generated from *Prochlorococcus* cultures. Therefore, carbohydrates and proteins with numerous and well-ordered hydrophilic functional groups may determine the ice nucleation potential of organic sea spray aerosols.

# Contents

<b>1</b>	<b>Introduction</b>	<b>3</b>
<b>2</b>	<b>Methods</b>	<b>5</b>
2.1	Chemical Representation and Culturing of <i>Prochlorococcus</i> . . . . .	5
2.2	Instrumentation . . . . .	5
2.2.1	Aerosol Generation - Frit Bubbler . . . . .	5
2.2.2	Aerosol Generation - Atomizer . . . . .	6
2.2.3	SPectrometer for Ice Nuclei . . . . .	7
2.2.4	Particle Analysis by Laser Mass Spectrometry . . . . .	8
2.2.5	Differential Mobility Analyzer . . . . .	9
2.2.6	Condensation Particle Counter . . . . .	9
2.3	Experimental Setup . . . . .	9
<b>3</b>	<b>Results</b>	<b>10</b>
3.1	Chemical Composition of SSA Samples . . . . .	10
3.2	Ice Nucleation Properties of Organic Components . . . . .	13
<b>4</b>	<b>Discussion</b>	<b>15</b>
4.1	SSA Formation Mechanism Impact on Chemical Composition . . . . .	15
4.2	Effect of SSA Composition on Ice Nucleation Potential . . . . .	16
4.3	Broader Implications of SSA on Global Ice Nucleation . . . . .	17
<b>5</b>	<b>Conclusion</b>	<b>18</b>
<b>6</b>	<b>References</b>	<b>19</b>
	<b>Appendix A</b>	<b>24</b>
	<b>Appendix B</b>	<b>25</b>

# 1 Introduction

Atmospheric aerosols have a profound impact on climate by directly interacting with incoming solar radiation, as well as by serving as the seeds that nucleate clouds (Haywood and Boucher, 2000). Atmospheric aerosols come from a wide variety of natural and anthropogenic sources and have typical radii ranging from 0.001 to 10 micrometers (Haywood and Boucher, 2000). Regional air quality and global climate are both impacted by the presence of these particles. Unlike greenhouse gas emissions which have exacerbated the warming trends of climate change, aerosols are predicted to have a net cooling effect on the climate (IPCC 2014). However, there exist large uncertainties in the magnitude and the direction of the forcing that aerosol indirect effects have on Earth's radiation budget (IPCC 2014). The subjective confidence level of IPCC Fifth Assessment Report was "low" for cloud adjustments due to aerosols (IPCC 2014). Understanding aerosol-cloud relationships is vital to reducing the uncertainty present in climate models and forecasts (IPCC 2014).

Atmospheric aerosol particles act as centers for water droplet or ice crystal nucleation. Many types of particles found in the atmosphere act as cloud condensation nuclei, which are the surfaces upon which water makes the transition from a vapor to a liquid to form a cloud droplet. A small subset of the atmospheric aerosol population can induce ice formation at conditions under which ice would not form without them (Hoose and Möhler, 2012). Only approximately one in  $10^5$  aerosol particles can act as these ice nucleating particles (INPs), which are the foundation for the formation of ice crystals (Pruppacher and Klett, 2011; DeMott et al., 2003; Rogers et al., 1988). Activated INPs can go on to form high-altitude tropospheric ice clouds, referred to as cirrus clouds, and additionally contribute to mixed-phase cloud glaciation, which are important factors in global climate (DeMott et al., 2003; Rossow and Schiffer, 1999). The potential of different types of aerosols to act as INPs is not well documented (Hoose and Möhler, 2012). Until empirical tests on nucleation ability are done, predicting which particles will nucleate ice is impossible.

Temperature and saturation ratio with respect to ice are the main environmental factors which determine the mechanism of ice nucleation (Hoose and Möhler, 2012). Ice can form in clouds without the presence of INPs through homogeneous freezing of water and solution droplets at high ice supersaturation and at temperatures below  $-38^{\circ}\text{C}$  (Koop, 2000). The specific onset point of nucleation is a function of the water activity of the solution under consideration (Koop, 2000). Homogeneous freezing requires soluble components of a given aerosol to deliquesce, or take up water below 100% relative humidity. After deliquescence occurs, the liquid water can freeze spontaneously given the low temperatures.

Alternatively, heterogeneous ice nucleation requires preexisting INPs in order to occur (Cziczo et al., 2013). Heterogeneous ice nucleation is thermodynamically assisted by the presence of INPs so that nucleation takes place at lower supersaturations or warmer temperatures than are required for homogeneous ice nucleation (Vali et al., 2015). Ambient temperature, relative humidity, and the physical and chemical properties of aerosol particles impact the concentrations of heterogeneous INPs in the upper troposphere (DeMott et al., 2003). Depositional nucleation occurs when ice forms directly from water vapor onto INPs, a process which occurs in cirrus clouds (Pruppacher and Klett, 2011). Other heterogeneous nucleation processes occur in supercooled liquid environments, such as mixed-phase clouds. These modes include condensation freezing, in which water vapor condenses on INPs at below freezing temperatures to form a liquid droplet which freezes instantaneously; immersion freezing, in which INPs act as cloud condensation nuclei and the formed droplet freezes when the temperature is lowered; and contact freezing, in which a particle comes into contact with the supercooled water phase and induces freezing (Pruppacher and Klett, 2011).

Like all aerosols, some INPs have natural sources, such as desert dust, pollen, or marine plankton, while others have anthropogenic sources (Vali et al., 2013). However, the largest

natural source of atmospheric aerosol by emissions is sea spray (Erickson and Duce, 1988). Sea spray aerosols (SSA), which have total global emissions estimated to be  $1-3 \times 10^{16}$  g per year, exhibit a wide variety of chemical and physical properties. There are multiple modes of aerosol production through sea spray, but two produce aerosol particles small enough to last in the atmosphere: bubble bursting and jet drops. The particles generated in both of these production methods can act as cloud condensation nuclei in the lower troposphere, and some as INPs if they are transported into the upper troposphere (Feingold et al., 1999, Carrio et al., 2007).

Figure 1 shows an idealized view of SSA generation in the ocean. When particles are produced through bubble bursting, bubbles created by cresting waves rise to the surface of the water and pop, sending submicron pieces of the film of the bubble up to 20 centimeters into the air (Blanchard, 1963). Meanwhile, jet drop formation occurs when the crater in the ocean surface left by the bursting bubble fills, producing a central jet which ejects droplets which are larger than the aerosols produced by bubble bursting. Both of these aerosol production methods may result in the presence of marine organic matter in the atmosphere. For bubble bursting, the bubbles typically have an organically-enriched film of small hydrophobic organics from lysed cells and vesicles. When the bubble bursts, fragments of the organic film are ejected into the atmosphere (Zhuang et al., 1993). In jet droplet aerosol formation, larger portions of cells and vesicles can be sent into the atmosphere along with other inorganic components present in bulk seawater (Bigg and Leck, 2008; Collins et al., 2014).

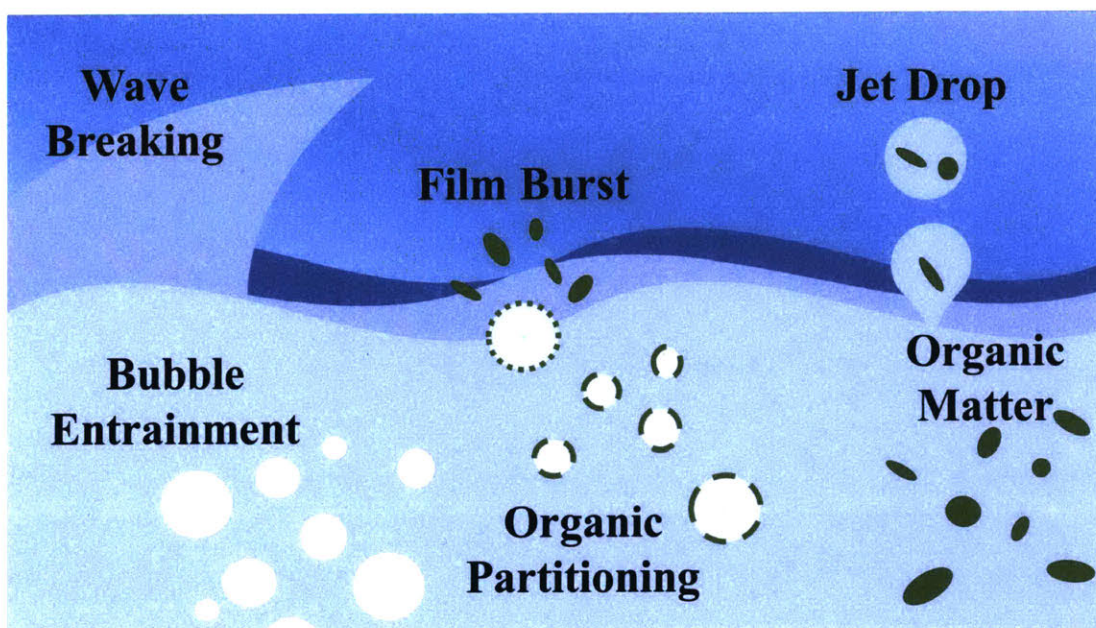


Figure 1: *Idealized schematic of SSA generation.* Breaking waves entrain bubbles below the sea surface. These bubbles take up organic matter which is present in the sea surface microlayer and subsurface water. At the surface, the organically enriched film of the bubble bursts, resulting in small film burst particles. The crater left by the popped bubble fills with subsurface water, resulting in the discharge of jet drop particles.

Current research focuses mainly on the role of SSA as INPs through condensation and immersion freezing (DeMott et al., 2016; Junge and Swanson, 2008). Limited data exist regarding the role of deposition freezing for the same particles. SSA can homogeneously nucleate ice well because the presence of salts allows the particle to deliquesce, taking up water before the relative humidity reaches above 100%. Additionally, the porosity of organically enriched SSA may enable these particles to nucleate ice depositionally (Adler et al., 2013). The increased porosity of the aerosols in high-altitude clouds results from phase separation upon freezing followed by a glass



transition of the organic material. A porous structure can be preserved after ice sublimation (Adler et al., 2013). The observed increase in ice nucleation efficiency of glassy organic particles present in high-altitude clouds may be explained by the presence of the porous structures.

We are studying how chemical composition of SSA impacts the ability of these aerosols to act as INPs. A continuous flow diffusion chamber is used to study how particles related to the marine cyanobacteria *Prochlorococcus* activate as INPs. *Prochlorococcus* is one of the most widespread and abundant marine primary producers and is used as a representative source of organic SSA (Flombaum et al., 2013). In addition, we use a single particle mass spectrometer to investigate how the chemical composition of SSA impacts ice nucleation potential. Ice nucleation potential is the likelihood of a particle to nucleate ice under certain conditions and is characterized by temperature and supersaturation at nucleation onset. By exposing the lysed cells and analogues of *Prochlorococcus*'s organic components to a range of tropospheric-relevant temperatures and ice supersaturations consistent with heterogeneous freezing, we begin to determine the ice nucleation potential of laboratory-generated SSA.

## 2 Methods

### 2.1 Chemical Representation and Culturing of *Prochlorococcus*

Inorganic components of SSA were replicated using solutions of NaCl ( $\geq 99.9\%$ , Macron Chemical) and synthetic seawater (SSW; Paragon Scientific). The major inorganic salts of natural seawater (NaCl, MgCl<sub>2</sub>, KCl, CaSO<sub>4</sub>, and NaHCO<sub>3</sub>) are present in SSW. Particles of single component organics were generated from compounds representative of proteins, lipids, and carbohydrates found in natural SSA. Proteins were represented by bovine serum albumin (BSA;  $\geq 99\%$ , protease and fatty acid free), L-threonine ( $\geq 99\%$ ), L-arginine ( $\geq 99\%$ ), and L-aspartic acid ( $\geq 98\%$ ). Lipids were represented by stearic acid ( $\geq 98.5\%$ ), oleic acid ( $\geq 99\%$ ), elaidic acid ( $\geq 98\%$ ), and 1,2-decanediol ( $\geq 99\%$ ). The carbohydrates were represented by amylopectin ( $\geq 99\%$ ), D-(+)-trehalose ( $\geq 99\%$ ), D-(+)-raffinose ( $\geq 99\%$ ), and agarose ( $\geq 99.5\%$ ).

The phytoplankton *Prochlorococcus* was used to represent the sources of organic carbon in the global ocean. One of the most abundant marine cyanobacteria, *Prochlorococcus* are found across many ocean regions in global mean abundances of  $2.9 \times 10^{27}$  cells (Flombaum et al. 2013). The organisms are typically found in the upper water column, making them suitable for this study's interests in the organic components of the ocean surface microlayer (Flombaum et al., 2013). To grow cultures of the phytoplankton, two strains of phenotypically distinct high-light adapted *Prochlorococcus* (MED4 HLI and MIT9312 HLII) and one strain of a low-light adapted ecotype (NATL2A LL) were cultured axenically, or free from the presence of other organisms. The culturing occurred in a natural seawater based PRO99 liquid medium with a 13:11 Light:Dark incubator at 24°C (Moore et al., 2007). The cultures were harvested in the late exponential growth phase. In order to mechanically break apart the cells, some cell cultures were lysed by immersion in a pulsing sonicator for five minutes before aerosolization.

### 2.2 Instrumentation

#### 2.2.1 Aerosol Generation - Frit Bubbler

A bubbler allows for the generation of aerosols by bubbling filtered air through sintered glass into a solution. The rate of the airflow and the sinter pore size determine the size of the bubbles. It is not always possible to examine SSA in its natural state, so the bubbling method is one way to simulate seawater aerosolization in a laboratory setting. A wave tank is another aerosolization method. Our wave tank was constructed using a large flat-bottomed flask attached to a 0.5 - 5 Hertz shaker table. Splashing motions create aerosol particles, yet the total concentration of particles produced is an order of magnitude less than with the bubbler.

The employed generation method for this study had to accurately recreate the production of aerosols through both the film burst and jet drop modes. Figure 2 shows size distributions of SSA collected from field studies in the North Atlantic Ocean (Koponen et al. 2002), the tropical Atlantic Ocean (Atmospheric Radiation Measurement Climate Research Facility, 2014), and the tropical North Pacific Ocean (Marine Atmospheric radiation measurement Global energy and water cycle experiment cloud system study pacific cross section intercomparison Investigations of Clouds (MAGIC) campaign (Lewis et al., 2012)). Overlaid are size distributions from this study's particle generation using a frit bubbler, a wave tank, and from the Scripps Institute for Oceanography (SIO) Hydraulics Laboratory generation using a wave tank (Stokes et al., 2013). The bubbler was able to most accurately recreate the size distribution, and likely the chemistry, of natural SSA. We attribute the bimodality of the size distributions to the film burst particle (100-200 nm) and jet drop particle (400-600 nm) production mechanisms (Wang et al., 2017). The wave tank method was not able to recreate the two desired mechanisms and did not show a bimodal distribution which is seen in natural SSA. Out of the tested methods of aerosol generation, the bubbler most accurately recreated the size distribution of the natural SSA. We therefore used the bubbler to aerosolize cultures of *Prochlorococcus*.

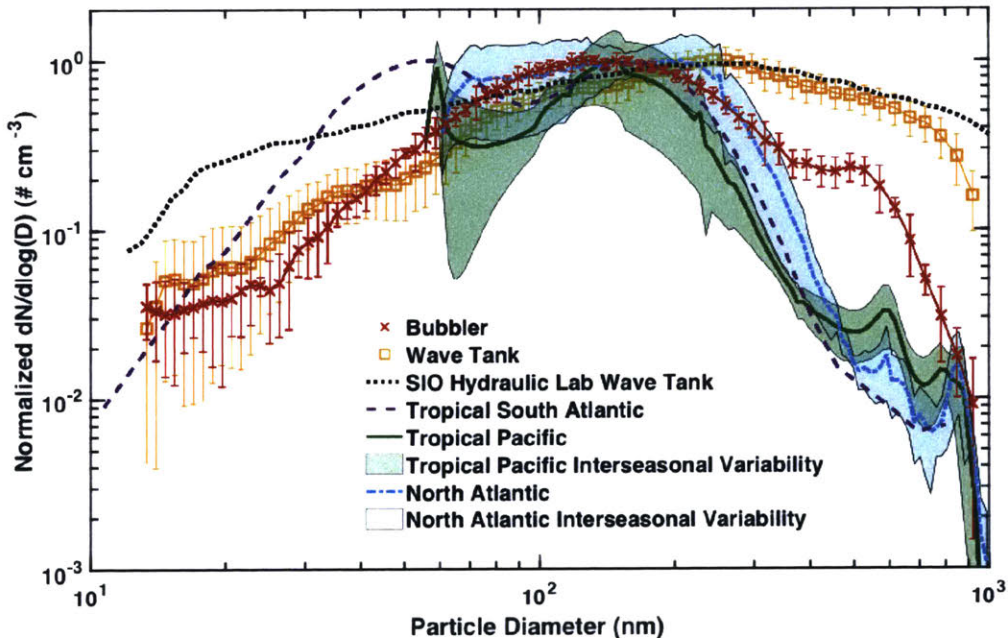


Figure 2: *Size distributions of particle concentration versus particle diameter for field and laboratory data.* Field measurements are reported from the Tropical South Atlantic (Koponen et al., 2002), Tropical Pacific (Lewis et al., 2012), and the North Atlantic (Atmospheric Radiation Measurement Climate Research Facility, 2014). Wave tank data are reported from the Scripps Institute for Oceanography Hydraulic Lab Wave Tank (Stokes et al., 2013). Reproduced from Wolf et al. (submitted).

### 2.2.2 Aerosol Generation - Atomizer

The atomizer also produces aerosol from a solution. Compressed air draws bulk liquid from a reservoir as a result of the Bernoulli effect. The high-velocity air breaks apart the liquid solution and the resulting droplets are suspended to form an aerosol. By varying the pressure of the compressed air or the dilution ratio of the solution, one can modify the resulting particle size distribution. (Baron and Willeke, 2001) The aerosolization method is typically used in the case when a given solution cannot be aerosolized using the bubbler because of its viscosity.



### 2.2.3 SPectrometer for Ice Nuclei

The SPectrometer for Ice Nuclei (SPIN; Droplet Measurement Technologies, Boulder, CO) is a continuous flow diffusion chamber (CFDC) instrument (described in Rogers, 1988) for studying the ice nucleation properties of aerosols. SPIN quantifies the concentrations of ice nucleating particles by controlling the temperature and relative humidity to which aerosol particles of interest are exposed (Garimella et al., 2016). Particles enter SPIN through an inlet and then pass between two walls coated with approximately 1 mm ice and separated by 1 cm. A sheath flow of about 9 liters per minute (lpm) constrains a laminar particle flow of 1 lpm to the center of the chamber. As shown in Figure 3, the walls are held at different temperatures to cause water vapor and heat to diffuse from the warmer wall to the colder wall. The magnitude of the temperature gradient determines the degree of ice supersaturation, with the maximum in supersaturation occurring near the center of the chamber (Rogers, 1988). For a typical experiment, the supersaturation within SPIN changes at a rate of approximately 2% relative humidity with respect to ice per minute. A full air and water flow diagram of SPIN can be found in the Appendix.

Within the chamber, some INPs will nucleate ice while other particles will pass through unactivated. Particles then enter the evaporation section of the instrument which is held at ice saturation. Here, ice particles stay as ice but liquid water is evaporated from droplets which have not nucleated ice. At the bottom of SPIN is an Optical Particle Counter which outputs data about the size and polarization properties of the individual particles which pass through it. The values of the polarization properties describe whether a particle has nucleated ice or has remained unactivated. Garimella et al. (2016) describes a constructed machine learning algorithm which trains on the four polarization parameters to create probability density functions for ice crystals, water droplets, and unactivated aerosols. Individual particles can then be classified into their respective phases.

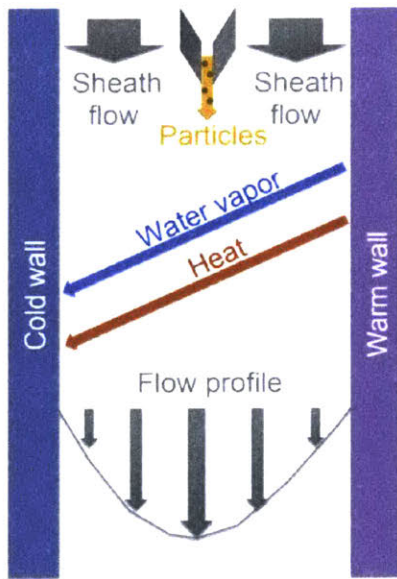


Figure 3: **Representation of an idealized CFDC.** A flow of particles passes between two ice-coated walls which are held at different temperatures. The difference in temperature between the two walls results in water vapor and heat diffusion from the warm wall to the cold wall. Supersaturation exists at a maximum near the centerline of the chamber. The particle flow is between two sheath flows along the walls, restricting the particles to the supersaturation maximum at the central lamina. Figure adapted from Garimella et al. (2017).

Garimella et al. (2017) describes the tendency for particles within a CFDC instrument to spread outside the center lamina, where ice supersaturation is greatest. Through timed pulse experiments under conditions comparable to the ones being tested, the fraction of aerosols constrained to the center lamina were calculated. Figure 4 shows the fraction of aerosols in the lamina flow as a function of the ice saturation ratio in SPIN at five different temperatures. In the ideal case, when all particles are constrained within the laminar flow, all of the data



points would form a horizontal line at 1.0. However, the fraction of particles in the lamina is much lower than 1.0 at the given temperatures and total flow of 9.8 L min<sup>-1</sup>. As particles outside the lamina experience a lower supersaturation and are unlikely to activate, a correction factor between 1.86 and 7.96 should be applied to fractional activation data derived assuming all particles are constrained to the lamina. A correction factor is calculated by taking the inverse of the fraction of particles in the lamina at a specific temperature and supersaturation.

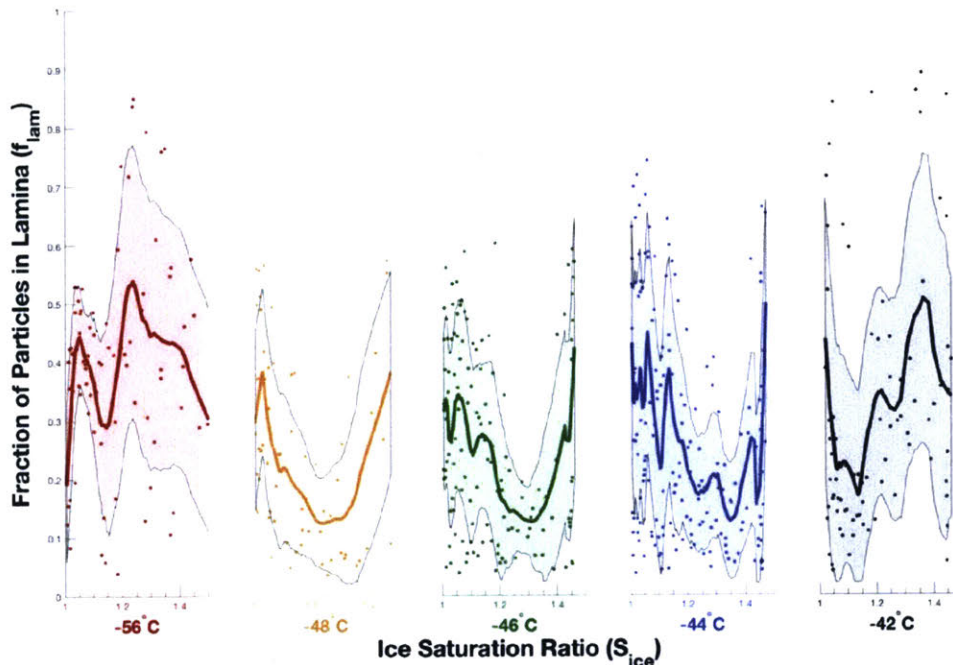


Figure 4: *Particle lamina spreading in SPIN.* The fraction of particles constrained to the SPIN aerosol lamina ( $f_{lam}$ ) as a function of ice saturation ratio ( $S_{ice}$ ) is represented across temperatures relevant to this study (-56 to -42° C). One standard deviation in variability is represented by the shaded regions and points represent individual measurements. A correction factor for fractional activation is obtained by taking the inverse of  $f_{lam}$  at a specified temperature and  $S_{ice}$ . Adapted from Wolf et al. (submitted).

#### 2.2.4 Particle Analysis by Laser Mass Spectrometry

The Particle Analysis by Laser Mass Spectrometry (PALMS) instrument is a single particle mass spectrometer described in detail by Thomson et al. (1997) and Cziczo et al. (2006). Aerosol particles are drawn by vacuum into PALMS, with a typical size sampling range between 0.1-1.5 micrometers (Cziczo et al., 2006). A fraction of the indrawn particles is sized by two 532 nm neodymium yttrium aluminum-garnet lasers using the particle transit time between the two laser beams. A 193 nm excimer laser then vaporizes and ionizes the particles and the atomic and molecular ions travel into a time of flight mass spectrometer which records their mass-to-charge ratio. Since multiple charges are rare with the PALMS excimer laser, the resulting mass-to-charge ratios are equivalent to particle mass. The spectrometer collects either positive or negative ion spectra for the particles (DeMott et al., 2003). Particle ionization within PALMS is not quantitative, meaning that individual particles from the same stream may show widely contrasting chemical compositions. Therefore, large numbers of spectra have to be collected in order to perform statistical analysis on the chemical composition of particles. A full schematic diagram of PALMS can be found in the Appendix.

### 2.2.5 Differential Mobility Analyzer

A Differential Mobility Analyzer (DMA; Brechtel Manufacturing Inc., Hayward, CA) uses the electrical mobility of particles to guide particle size-selection. A particle's electrical mobility is primarily a function of its size and charge and is used to measure the ability of a particle to travel across an electric field. Within the DMA, aerosols pass through a neutralizer which gives the stream of aerosols a known electrostatic charge distribution. The stream of charged particles then travels through sheath air (5-8 lpm) and enters into an electric field (0-6000 V). Changing the electric field strength and the sheath air flow rate allows for the separation of particles of a particular electrical mobility, and therefore of a known size range.

### 2.2.6 Condensation Particle Counter

A Condensation Particle Counter (CPC; Brechtel Manufacturing Inc., Hayward, CA) is used to count aerosols when they are too small to be detected using traditional optical techniques. The working liquid (typically butanol) rests on top of a heated saturation block, generating a high vapor content of the solution in the chamber. The particles entering the CPC come into contact with the vaporized working liquid and then enter a cooled chamber, in which the difference in temperature results in supersaturation. The supersaturation causes the particles to act as condensation nuclei and to grow in size as they attract the vapor. The grown particles can then be detected by shining a light emitting diode through the sample and detecting and recording light scattering. The greater the difference in temperature between the heated chamber and the cooled chamber, the smaller the particles that can be counted.

## 2.3 Experimental Setup

Figure 5 shows a schematic of the experimental setup for a typical experiment. Initially, particles were generated with either a bubbler or an atomizer with a flow of 1.3 lpm provided by dry nitrogen air. The aerosol stream was further dried by passing through driers which uptook excess water from the particles. The stream then passed through the DMA, which size-selected particles. Particles thought to result from film burst generation were size selected at 200 nm, jet drop particles at 500 nm, and pure organic molecules at 100 nm. Because a large concentration of particles is necessary for there to be ice nucleation with these organic materials, the DMA may not work as effectively on a single-particle basis and therefore potentially allowed some doubly-charged large particles through. In addition, in some cases in which aerosol generation was low, a polydisperse (non-size selected) distribution of aerosols was necessary. In these polydisperse cases, the DMA was not used to size-select the generated particles.

A 0.3 lpm stream of the size-selected particles then traveled through the CPC, providing a total count of the number of particles of all sizes. SPIN sampled the remaining 1.0 slpm of the particle stream. From the CPC and SPIN data, the fractional activation of particles which activated as INPs was calculated. In order to obtain chemical composition data, the stream of size-selected particles could also be sent to PALMS at a flow rate of 0.3 lpm.

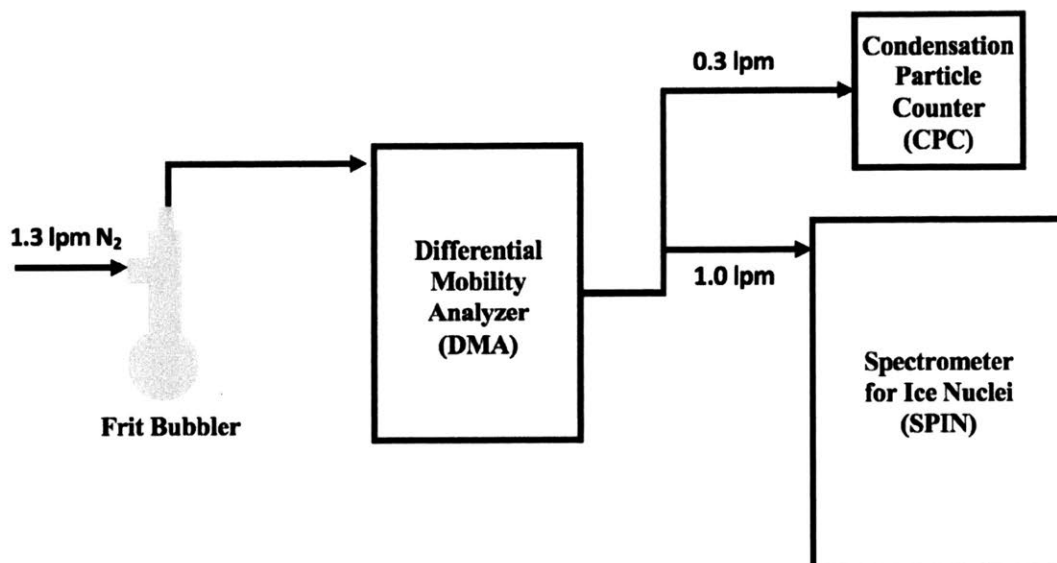


Figure 5: *Schematic of the typical experimental setup.* 1.3 lpm of dry lab air entered the frit bubbler, which contained the solution to be aerosolized. The resulting particle stream passed through the DMA, which size selected the appropriately-sized particles. 0.3 lpm of the stream passed to the CPC, where the total number of particles were counted. The remaining 1.0 lpm of the stream passed through to SPIN. Alternatively, the flow from the DMA could travel directly to PALMS.

### 3 Results

#### 3.1 Chemical Composition of SSA Samples

Characteristic negative PALMS mass spectrometry spectra for synthetic seawater (SSW), the *Prochlorococcus* culturing medium (Pro99), and 200 and 500 nm particles from lysed *Prochlorococcus* cultures are shown in Figure 6. The spectrum for SSW shows large peaks at ion mass/charge ( $m/z$ ) ratios of 35 and 37, corresponding to chlorine isotopes. Most of the ion peaks in the SSW spectrum are inorganic in nature. There is very little carbon signal in the SSW, and that which may be present is indistinguishable as a signal in the background noise from the spectra.

Overall, the culturing medium ion spectrum resembles that of the SSW. The limited carbon (peak at  $C_2^-$   $m/z = 24$ ) present in the culturing medium may relate to chelating agents used to keep metallic nutrients suspended in the solution (Moore et al., 2007). However, the culturing medium shows reduced sulfate and sulfite ion signals compared to the SSW.

In contrast, the spectra of the lysed and aerosolized *Prochlorococcus* cultures show strong ion signals corresponding to carbon-containing compounds. The 200 nm film burst particles demonstrate strong carbon signals ( $C^-$   $m/z = 12, 13$ ;  $C_2^-$   $m/z = 24, 25$ ;  $CN^-$   $m/z = 26$ ,  $CNO^-$   $m/z = 42, 44$ ; and  $C_4^-$   $m/z = 48$ ). Meanwhile, the 500 nm jet drop particles showed lower carbon, phosphorus ( $PO_2^-$   $m/z = 63$ ;  $PO_3^-$   $m/z = 79$ ; and  $PO_4^-$   $m/z = 95$ ), and nitrogen ( $NO^-$   $m/z = 26$ ) signals. Nitrogen is found in amine functional groups while phosphorus is present in the phosphate backbones of nucleic acids and headgroups of phospholipids. The nitrogen and phosphorus present in the jet drop particles may result from the ionization of these biochemical components.



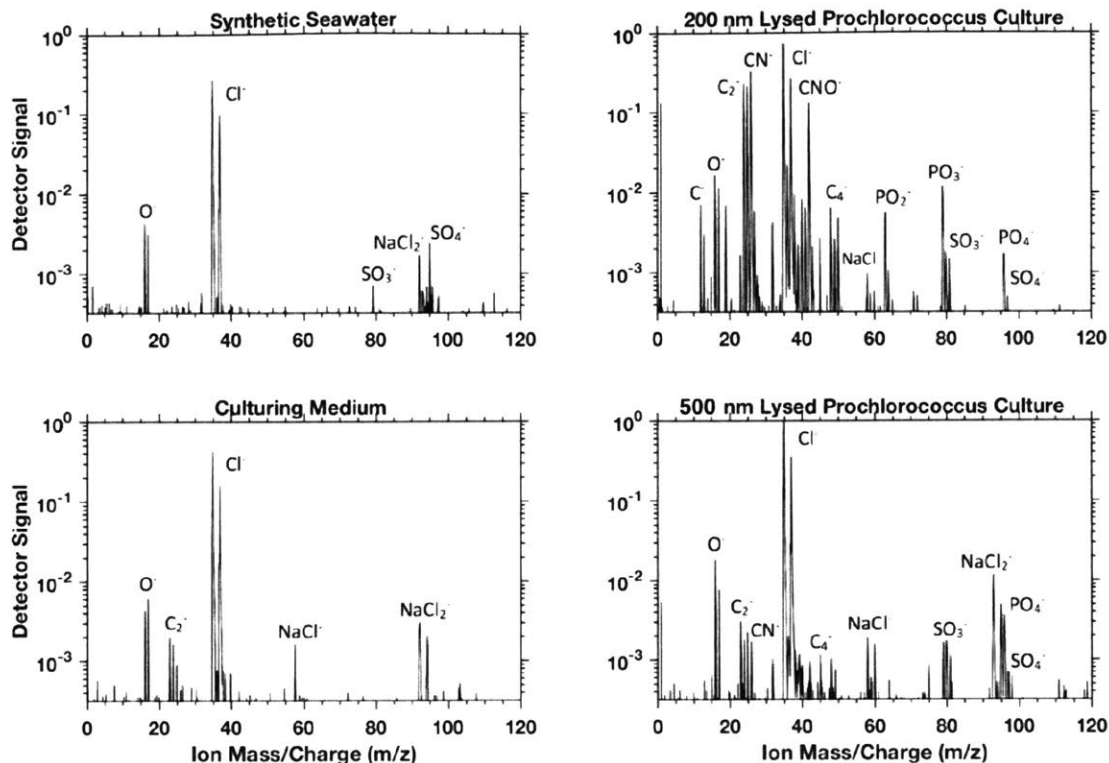


Figure 6: **Particle mass spectra.** Negative characteristic spectra from PALMS are shown for synthetic seawater, *Prochlorococcus* culturing medium (Pro99), and 200 and 500 nm particles lysed *Prochlorococcus* cultures.

Carbon and chlorine ion signal comparisons from over 750 PALMS spectra are shown for *Prochlorococcus* culturing medium and 200 and 500 nm particles from lysed *Prochlorococcus* cultures in Figure 7. The carbon signal is expected to correlate to organic mass fraction while the chlorine signal corresponds to inorganic components of the sample. The carbon ion signal for the culturing medium is low to zero in almost every sample. However, the aerosols generated from the lysed cultures, especially the 200 nm particles, demonstrate a larger signal of carbon. As the signal of the organic carbon increases in the samples, the signal of the inorganic chlorine decreases.

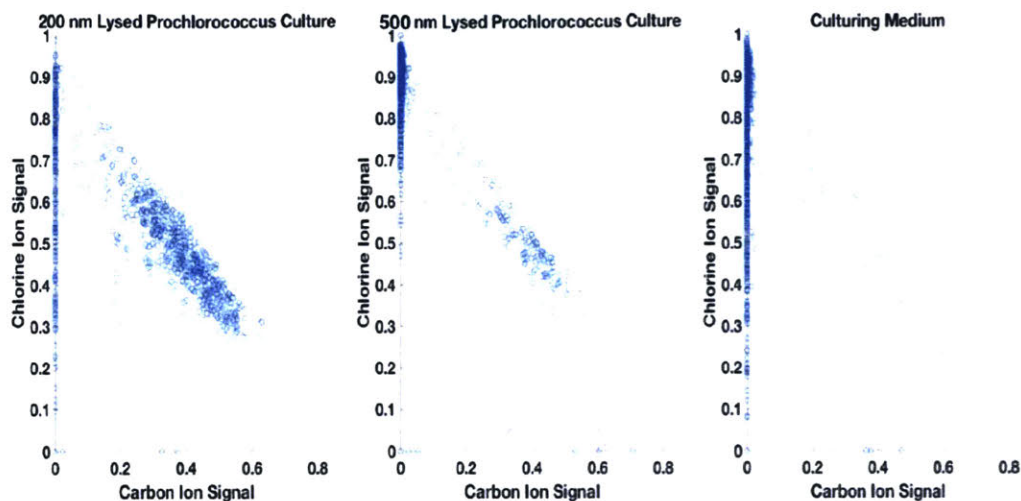


Figure 7: *Carbon and chlorine ion signal comparisons of lysed Prochlorococcus cultures.* Comparisons of ion signals organic carbon (ion  $m/z$  of 12, 13, 24, 25, 26, 28, 38, 42, 44, and 48) and chlorine (ion  $m/z$  of 35 and 37) are shown for >750 samples of Prochlorococcus culturing medium (Pro99) and 200 and 500 nm particles from lysed Prochlorococcus (NATL2A) cultures.

Figure 8 shows carbon and chlorine ion signal comparisons of water samples collected from the Straits of Florida in March 2018. The particles generated from the water sampled from the organically enriched sea surface microlayer demonstrate stronger carbon signals than those generated from the water sampled from the subsurface, two meters down. These results correlate to those shown in Figure 7. The smaller particles suspected to form from bubble bursting at the ocean surface, where the sea surface microlayer exists, have more organic carbon than the larger particles formed from the jet drop mechanism, which aerosolizes subsurface water. This comparison suggests that the laboratory analogue to seawater using *Prochlorococcus* and the two SSA generation mechanisms employed in this study were effective in mimicking the chemical composition natural seawater.

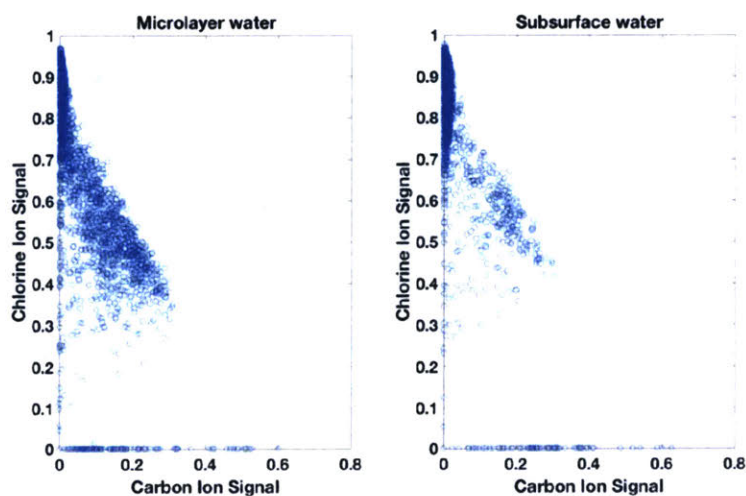


Figure 8: *Carbon and chlorine ion signal comparisons of field samples.* Comparisons of ion signals organic carbon (ion  $m/z$  of 12, 13, 24, 25, 26, 28, 38, 42, 44, and 48) and chlorine (ion  $m/z$  of 35 and 37) are shown for samples of a) sea surface microlayer and b) subsurface water collected from the Straits of Florida.

### 3.2 Ice Nucleation Properties of Organic Components

The supersaturation with respect to ice ( $S_{ice}$ ) at the onset of ice nucleation for inorganic, protein, lipid, carbohydrate, and *Prochlorococcus* particles is shown in Figure 9. The onset of nucleation is defined as when 1 in  $10^4$  particles activated as an INP. Correction for the lamina spreading in SPIN (Figure 5) was implemented. Each condition was replicated at least twice and the points represent the average of the trials conducted at that temperature. The black line corresponds to homogeneous nucleation, as defined in Koop et al. (2000), the  $S_{ice}$  at which ice crystals nucleate due to chance aggregation of liquid molecules. None of the groups of particles followed uniform patterns of nucleation and all of the tested samples nucleated homogeneously above  $-43^\circ\text{C}$ .

The inorganic particles generated from SSW and from the culturing medium solution primarily activated homogeneously. Some heterogeneous nucleation occurred around  $-55^\circ\text{C}$  but particles again nucleated homogeneously below  $-58^\circ\text{C}$ . Kong et al. (2018) provides an explanation for this phenomenon. Between  $-55$  and  $-58^\circ\text{C}$ , depositional freezing and deliquescence compete kinetically. Deliquescence leads to homogeneous freezing; however, between these temperatures, deposition nucleation is more favorable, even for purely inorganic substances (Kong et al., 2018). Other studies which tested the heterogeneous nucleation abilities of inorganic substances found similar results (Schill and Tolbert, 2014; Ladino et al., 2016).

Particles generated from proteins and amino acids demonstrated two modes of nucleation. The protein mixture (a combination of all of the tested protein substances in equal parts) and the aspartic acid were effective heterogeneous INPs. As the temperature got lower, the  $S_{ice}$  required to activate the particles lowered as well. The critical ice saturations for aspartic acid and the mixture were similar, suggesting that aspartic acid determined the nucleation potential of the mixture. Meanwhile, the threonine and bovine serum albumin did not activate heterogeneously until below  $-47^\circ\text{C}$  while the arginine solely activated homogeneously.

Some carbohydrates followed a similar pattern to the aspartic acid. Particles produced from two polysaccharides (amylopectin and agarose) were effective INPs below  $-46^\circ\text{C}$  while the oligosaccharide samples only nucleated homogeneously. The particles generated from lipids generally weakly nucleated ice below homogeneous freezing conditions. Oleic acid and the lipid mixture nucleated ice at  $S_{ice}$  values of 1.21 and 1.27 at approximately  $-56$  and  $-54^\circ\text{C}$ , respectively.

Different forms of particles generated from *Prochlorococcus* cultures were tested for their ice nucleation abilities. Jet drop (500 nm) particles demonstrated the lowest ice nucleation potential of the particles generated from cells, nucleating homogeneously until  $-49^\circ\text{C}$ , below which they nucleated between  $S_{ice}$  values of 1.32 and 1.36. Particles generated from whole cells nucleated homogeneously until  $-48^\circ\text{C}$  with only slightly more ability to nucleate heterogeneously than jet drop particles. Meanwhile, the film burst (200 nm) particles demonstrated effective INP properties below  $-44^\circ\text{C}$ . At  $-50^\circ\text{C}$ , the film burst particles activated at  $S_{ice} = 1.12$ . The polydisperse stream of particles demonstrated highly efficient INP properties. The behavior of the film burst and the polydisperse samples follow similar patterns between  $-40$  and  $-50^\circ\text{C}$ .



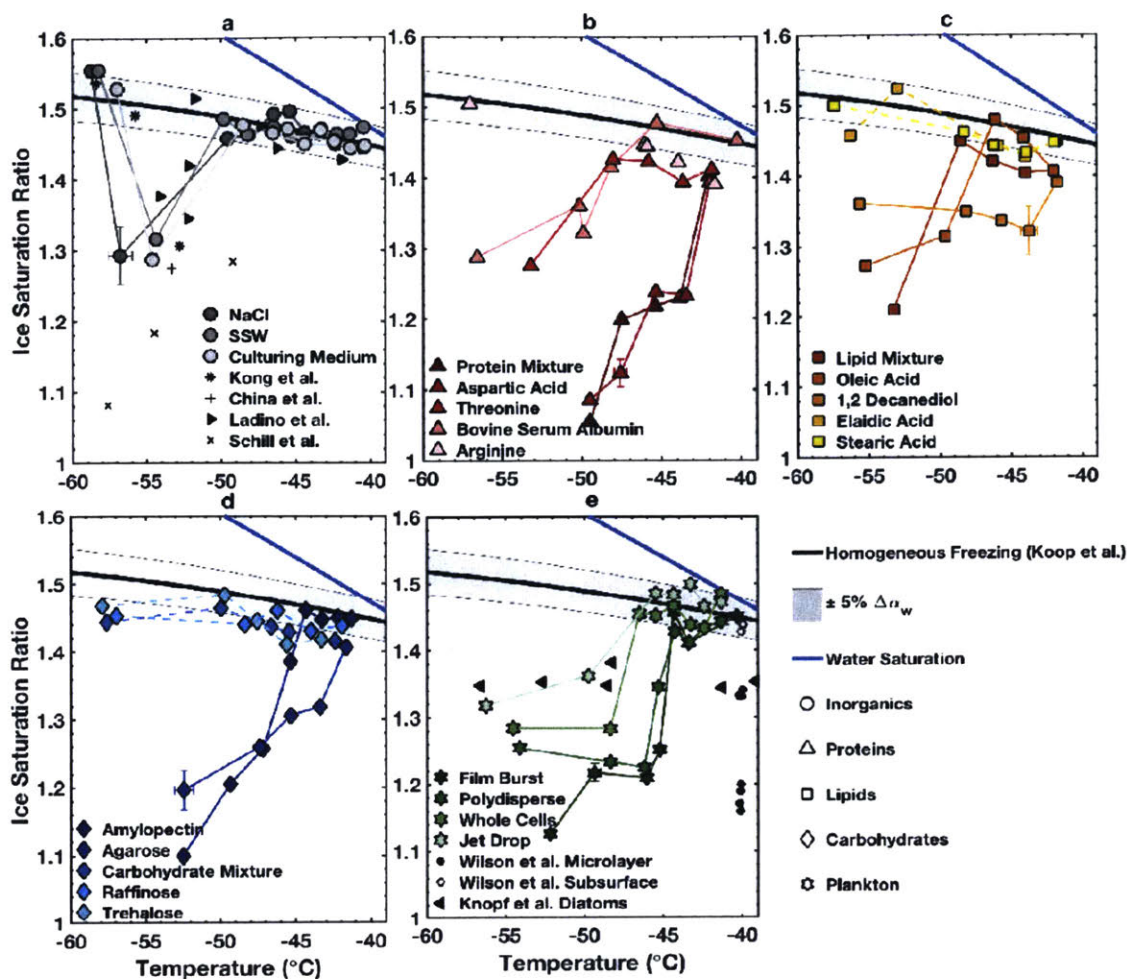


Figure 9: *Onset of ice nucleation.* The supersaturation with respect to ice at the onset of ice nucleation is shown for a) inorganics and culturing media, b) proteins, c) lipids, d) carbohydrates, and e) cultures of *Prochlorococcus*. Amylopectin, agarose, aspartic acid, and the protein mixture exhibited nucleation behaviors similar to the smaller particles generated from *Prochlorococcus* cultures. Reproduced from Wolf et al. (submitted).

The fractional activation as a function of  $S_{ice}$  at  $-46^\circ\text{C}$  is shown in Figure 10. Fractional activation demonstrates what percentage of particles have activated as ice at a given temperature. Higher fractional activation at lower ice supersaturation suggests the substance to be a good INP. The possible underactivation of particles due to lamina spreading is accounted for using the correction factor determined from Figure 5.

Particles derived from inorganics are ineffective INPs, demonstrating no activation until homogeneous conditions are reached. Aspartic acid is the only individual protein sample which exhibits heterogeneous nucleation. The protein mixture follows a similar trend. Lipids as a whole demonstrate high  $S_{ice}$  upon nucleation onset. Agarose and amylopectin demonstrated strong heterogeneous nucleation potential; however, the carbohydrate mixture did not. This idiosyncrasy is atypical, as the mixtures usually follow the potential of the most effective component. For the cells, the film burst and polydisperse particles exhibited strong heterogeneous nucleation potential, activating at  $S_{ice}$  values of 1.2 and 1.18, respectively.

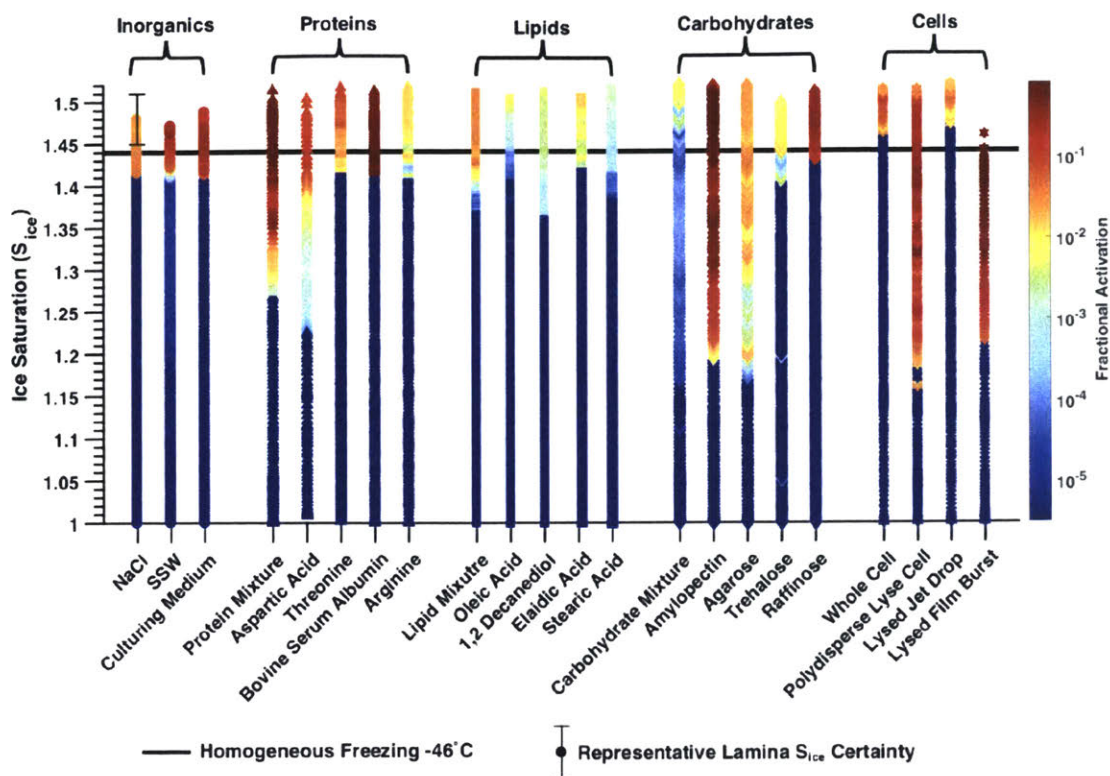


Figure 10: *Fractional ice activation.* The fraction of particles activated as ice as a function of  $S_{ice}$  is shown for the experiments run at  $-46^{\circ}C$ . Inorganics are poor INPs while aspartic acid, the protein mixture, agarose, and amylopectin effectively activated as INPs. The smaller particles produced from *Prochlorococcus* also demonstrated strong ice nucleation abilities. Reproduced from Wolf et al. (submitted).

## 4 Discussion

### 4.1 SSA Formation Mechanism Impact on Chemical Composition

The compositional differences between the film burst and the jet drop particles suggests that the differences in generation of the two particle types result in different values of organic enrichment. The synthetic seawater and culturing medium have very little organic content, reflected by the low organic signal of aerosols generated from these solutions (Figure 7). Meanwhile, both of the particle types generated from lysed *Prochlorococcus* cells contain organic material. The smaller film burst particles are more organically enriched than the larger jet drop particles. The organic microlayer across the ocean surface from which film burst particles arise contains more organic material which is relevant for ice nucleation than the deeper subsurface water from which jet drop particles form (Wilson et al., 2015).

The organic components present in the jet drop and film burst particles cannot be identified directly, only in terms of relative abundance. However, the relative organic enrichment of the film burst particles demonstrates that the different modes of generation are important in creating distinguishing differences within particles considered bulk SSA. Overall, the different sizes and compositions of these particles suggests that SSA generation must be considered and replicated accurately when testing the ice nucleation properties of natural sea spray aerosols in a laboratory setting. The organic enrichment of film burst particles may also be important in contexts outside of ice nucleation. For instance, Salter et al. (2016) suggests that calcium enrichment in SSA may

be important for the pH-dependent aqueous chemistry of marine aerosols due to contributions to excess alkalinity.

## 4.2 Effect of SSA Composition on Ice Nucleation Potential

Amylopectin, agarose, aspartic acid, and the protein mixture most closely mimicked the nucleation behavior of the lysed *Prochlorococcus* film burst particles. This trend suggests that the presence of certain carbohydrate and protein molecules determine the heterogeneous ice nucleation onset of natural sea spray.

Amylopectin and agarose are both polysaccharides and show a steep decline of supersaturation at nucleation onset below  $-45^{\circ}\text{C}$ . The large chain-building structure and atomic orientation of these molecules may explain their ability to effectively act as INPs. Both of these molecules have many exposed hydroxyl groups which can act as sites for hydrogen bonding with water and other molecules. The liquid water which is attracted to these sites can form a critical ice embryo, with the particle acting as an INP. The hydroxyl groups contribute to the surface area of the particle which can act as a critical ice embryo (Graether and Jia, 2001). Unlike other particles which bind to ice and inhibit further growth, the amylopectin and agarose present large ice-nucleating surfaces. If a particle's molecular structure contains sequences which align with ice lattice structure, a stable ice embryo can form, decreasing the activation barrier for ice nucleation (Pummer et al., 2015).

Some other saccharide compounds may not act as INPs because they too readily adsorb water (Peng et al., 2001; Chan et al., 2008). If a molecule attracts water and forms a thin liquid coat, depositional freezing will not occur. Although there are no literature values for the water adsorption qualities of raffinose and trehalose, the other tested carbohydrate compounds, they may have formed a water coat, causing them to deliquesce and to be incapable of freezing depositionally. The deliquescence may explain why the carbohydrate mixture did not follow the ice nucleation behavior of the good INPs but instead was nucleation-inhibited until values consistent with homogeneous freezing. However, some particles generated from the carbohydrate mixture did nucleate below homogeneous freezing values. Potentially these particles were predominantly composed of the polysaccharides, which prevented deliquescence and allowed for depositional nucleation.

Comparatively, the aspartic acid and protein mixture demonstrate a steep decline of supersaturation at nucleation onset below  $-42^{\circ}\text{C}$ , reaching an  $S_{\text{ice}}$  below 1.1 at  $-50^{\circ}\text{C}$ . Aspartic acid, like agarose and amylopectin, also has an exposed hydroxyl group. However, both threonine and arginine, other tested nucleic acids, also have exposed hydroxyl groups. It is important to consider atomic orientation as it relates to ice nucleation. Ice will only nucleate in specific orientations and incompatible alignments will inhibit or prevent ice crystal growth. INPs have molecular features, such as well-positioned and distanced hydroxyl groups, which contribute to their ability to nucleate ice (Pandey et al., 2016; Graether and Jia, 2001; Pummer et al., 2015). Aspartic acid's positioning of hydroxyl groups may contribute to its ability to nucleate ice. Unlike for the carbohydrates, the protein mixture followed the good INP ability of the aspartic acid, suggesting that the threonine and arginine did not limit the mixture with deliquescent behavior (Chan et al., 2005).

Considering fractional activation, although they were all good INPs, more agarose and amylopectin than aspartic acid activated at lower supersaturations. This finding suggests that the polysaccharides played the largest role in causing the SSA to activate as INPs. The long-chain polysaccharides have more hydroxyl sites, thousands per chain, which have the capability and orientation to act as hydrogen bonding sites. The organic enriched film burst particles likely rely on hydroxyl groups to act as sites upon which ice nucleation can occur.



### 4.3 Broader Implications of SSA on Global Ice Nucleation

The chemical composition and properties of marine aerosol can have important consequences for the climate properties of these particles. The partitioning of water-soluble and water-insoluble organic matter and the diversity of molecules within the organic fraction is dependent on the size of the particle (Facchini et al., 2008). Considering the multiple generation methods of SSA, the organic composition of particles is therefore likely related to the mechanism of particle generation: film burst or jet drop. Differences in organic enrichment can have impacts on the ice nucleation properties of a particle. Wang et al. (2015) found a correlation between aliphatic-rich species, or non-aromatic hydrocarbons, and concentrations of INPs in an experiment with natural marine phytoplankton blooms. These aliphatic-rich organics were most likely aerosolized via the bubble film burst mechanism. When testing a different bloom, there was no enrichment of aliphatic species and no associated rise in INP concentration, suggesting that the presence of these organic compounds was vital to the increase in concentration of INPs (Wang et al., 2015).

Changes in the marine system, such as ocean acidification and eutrophication resulting from a lack of dissolved oxygen, may impact the chemistry of SSA. The molecular diversity of the compounds which make up the organic component of SSA is linked to the presence of marine bacteria and phytoplankton, which can vary in time and space (Cochran et al., 2017). In addition, a mesocosm study performed by Galgani et al. (2014) suggests that ocean acidification may impact the chemical composition of the ocean's surface microlayer. Changes include higher concentrations of hydrophilic amino acids and lower concentrations of carbohydrates (Galgani et al., 2014). Such changes in organic composition at the surface microlayer can impact bacterial composition and concentration at the ocean surface by impacting pH and habitability. These changes would impact the potential of SSA film burst particles to activate as INPs. Rapid shifts in the conditions of the marine system resulting from anthropogenic impacts and emissions may cause a range of impacts on a variety of climate-related processes, including ice nucleation (Wurl et al., 2017).

Models demonstrate great uncertainties when it comes to ice nucleation by SSA. Although models take differences in sub-micron and fine emissions into account, the importance of organic matter enrichment in these models is still being defined (O'Dowd et al., 2008; Vignati et al., 2009). Current models assume particles arising from sea spray to be internally mixed, meaning the particles are chemically and physically homogeneous and reflect the average of all of the components, inorganic and organic (Lesins et al., 2002). However, our data suggest that SSA assemblages are less internally mixed than these models assume. It appears that the presence of a specific organic compound in a particle can highly impact that particle's ability to nucleate ice. Individual particle composition is important to consider in an externally mixed assemblage of particles as each particle can demonstrate different properties, effecting characteristics such as the ability to impact direct radiative forcing, as studied in Lesins et al. (2002) or ice nucleation.

Vergara-Temprado et al. (2017) demonstrates that global distribution of concentrations of INPs are better aligned with ambient concentrations of feldspar and marine organic aerosols than with theoretical descriptions of INPs by temperature or size. Similarly, Burrows et al. (2013) found strong regional differences in the importance of INPs coming from marine and dust sources. These studies suggest that INPs from different sources must be better understood in order to effectively model the aerosol-cloud-climate system; treating all INPs as one assemblage is imprecise and results in errors in climate sensitivity in models. This study attempted to present a more cohesive view of INPs arising from SSA. A better understanding of the ambient concentrations of the particles arising from sea spray with respect to chemical composition will contribute to better modeling of the population of INPs. In addition, it is important to consider that despite arising from the same source, film burst and jet drop particles demonstrated highly disparate heterogeneous ice nucleation properties. In order to accurately represent the role of SSA in global ice nucleation processes, models must begin to accommodate for the differences in size and chemical composition of particles generated from the same source.

## 5 Conclusion

In this study, we investigated the role of SSA chemical composition on heterogeneous ice nucleation behavior. SSA particles were generated in a laboratory setting using the naturally-abundant *Prochlorococcus* cyanobacteria as model source of marine organic matter. Particle generation from a frit bubbler resulted in the production of two kinds of particles, which were designated as smaller film burst particles and larger jet drop particles. The smaller film burst particles were organically enriched compared to the larger jet drop particles, as confirmed by mass spectrometry. The difference in chemical composition between the particles suggests further differences between the particles' abilities to activate as INPs.

The heterogeneous ice nucleation potentials of the SSA and relevant carbohydrates, proteins, and lipids were analyzed. Inorganic components were ineffective as INPs. Larger jet drop particles from the lysed *Prochlorococcus* cultures acted as INPs below  $-49^{\circ}\text{C}$ , while the smaller film burst particles were effective INPs at warm temperatures and low supersaturations at colder temperatures. Comparing the results of the SSA generated from lysed cell cultures to pure organic molecules found that the large polysaccharides agarose and amylopectin as well as aspartic acid (a nucleic acid) most closely mimicked the heterogeneous ice nucleation behavior of film burst particles. Nucleation was initiated at high temperatures and low supersaturations for colder temperatures for these molecules, suggesting an explanation for the good INP behavior documented in film burst particles. However, other organic substances were moderate or poor INPs. The presence and favorable orientation of hydroxyl groups in organic molecules appears to be an important factor in considering ice nucleation potential of film burst SSA particles.

Future work in this area should focus on confirming the difference in and importance of organic enrichment between different modes of SSA. Individual organic components, specifically carbohydrate and protein substances, should be isolated from natural sea spray and have their ice nucleation properties tested. Further data will help develop an understanding of the role SSA play in the larger aerosol-cloud-climate system. In addition, field research and further laboratory studies will establish how the nucleation behaviors of SSA may change as a result of the marine impacts of Earth's changing climate.

### Acknowledgements

I would like to thank my advisor Dr. Dan Cziczo for his support as a research supervisor. I would also like to thank Martin Wolf for his daily supervision and joy in sharing knowledge. Additionally, I would like to thank Jane Connor for her assistance in writing and preparing this report and its accompanying presentation. Finally, thank you to all of the members of the Cziczo Group and the MIT Department of Earth, Atmospheric, and Planetary Science for their encouragement and assistance throughout my undergraduate career. The MIT David P. Bacon Fund provided financial support for this project. The culturing of *Prochlorococcus* by the Chisholm Lab was supported by a grant from the National Science Foundation (OCE-1356460).

## 6 References

- Adler, Gabriela, Thomas Koop, Carynelisa Haspel, Ilya Taraniuk, Tamar Moise, Ilan Koren, Reuven H. Heiblum, and Yinon Rudich. 2013. "Formation of Highly Porous Aerosol Particles by Atmospheric Freeze-Drying in Ice Clouds." *Proceedings of the National Academy of Sciences* 110 (51): 20414–19. <https://doi.org/10.1073/pnas.1317209110>.
- Bigg, E. Keith, and Caroline Leck. 2008. "The Composition of Fragments of Bubbles Bursting at the Ocean Surface." *Journal of Geophysical Research: Atmospheres* 113 (D11): D11209. <https://doi.org/10.1029/2007JD009078>.
- Blanchard, Duncan C. 1963. "The Electrification of the Atmosphere by Particles from Bubbles in the Sea." *Progress in Oceanography* 1 (January): 73–202. [https://doi.org/10.1016/0079-6611\(63\)90004-1](https://doi.org/10.1016/0079-6611(63)90004-1).
- Burrows, S. M., C. Hoose, U. Pöschl, and M. G. Lawrence. 2013. "Ice Nuclei in Marine Air: Biogenic Particles or Dust?" *Atmos. Chem. Phys.* 13 (1): 245–67. <https://doi.org/10.5194/acp-13-245-2013>.
- Carrio, G. G., S. C. van den Heever, and W. R. Cotton. 2007. "Impacts of Nucleating Aerosol on Anvil-Cirrus Clouds: A Modeling Study." *Atmospheric Research* 84 (2): 111–31. <https://doi.org/10.1016/j.atmosres.2006.06.002>.
- Chen, Y. L., P. J. DeMott, S. M. Kreidenweis, D. C. Rogers, and D. E. Sherman. 2000. "Ice Formation by Sulfate and Sulfuric Acid Aerosol Particles under Upper-Tropospheric Conditions." *Journal of the Atmospheric Sciences* 57 (22): 3752–66. [https://doi.org/10.1175/1520-0469\(2000\)057<3752:IFBSAS>2.0.CO;2](https://doi.org/10.1175/1520-0469(2000)057<3752:IFBSAS>2.0.CO;2).
- Cochran, Richard E., Olga Laskina, Jonathan V. Trueblood, Armando D. Estillore, Holly S. Morris, Thilina Jayarathne, Camille M. Sultana, et al. 2017. "Molecular Diversity of Sea Spray Aerosol Particles: Impact of Ocean Biology on Particle Composition and Hygroscopicity." *Chem* 2 (5): 655–67. <https://doi.org/10.1016/j.chempr.2017.03.007>.
- Collins, D. B., D. F. Zhao, M. J. Ruppel, O. Laskina, J. R. Grandquist, R. L. Modini, M. D. Stokes, et al. 2014. "Direct Aerosol Chemical Composition Measurements to Evaluate the Physicochemical Differences between Controlled Sea Spray Aerosol Generation Schemes." *Atmos. Meas. Tech.* 7 (11): 3667–83. <https://doi.org/10.5194/amt-7-3667-2014>.
- Cziczo, D. J., P. J. DeMott, C. Brock, P. K. Hudson, B. Jesse, S. M. Kreidenweis, A. J. Prenni, J. Schreiner, D. S. Thomson, and D. M. Murphy. 2003. "A Method for Single Particle Mass Spectrometry of Ice Nuclei." *Aerosol Science and Technology* 37 (5): 460–70. <https://doi.org/10.1080/02786820300976>.
- Cziczo, Daniel J., Karl D. Froyd, Corinna Hoose, Eric J. Jensen, Minghui Diao, Mark A. Zondlo, Jessica B. Smith, Cynthia H. Twohy, and Daniel M. Murphy. 2013. "Clarifying the Dominant Sources and Mechanisms of Cirrus Cloud Formation." *Science* 340 (6138): 1320–24. <https://doi.org/10.1126/science.1234145>.
- Cziczo, Daniel J., David S. Thomson, Thomas L. Thompson, Paul J. DeMott, and Daniel M. Murphy. 2006. "Particle Analysis by Laser Mass Spectrometry (PALMS) Studies of Ice Nuclei and Other Low Number Density Particles." *International Journal of Mass Spectrometry*,



- DeMott, P. J., D. J. Cziczo, A. J. Prenni, D. M. Murphy, S. M. Kreidenweis, D. S. Thomson, R. Borys, and D. C. Rogers. 2003. “Measurements of the Concentration and Composition of Nuclei for Cirrus Formation.” *Proceedings of the National Academy of Sciences of the United States of America* 100 (25): 14655–60. <https://doi.org/10.1073/pnas.2532677100>.
- DeMott, Paul J., Thomas C. J. Hill, Christina S. McCluskey, Kimberly A. Prather, Douglas B. Collins, Ryan C. Sullivan, Matthew J. Ruppel, et al. 2016. “Sea Spray Aerosol as a Unique Source of Ice Nucleating Particles.” *Proceedings of the National Academy of Sciences* 113 (21): 5797–5803. <https://doi.org/10.1073/pnas.1514034112>.
- Deng, Chunhua, Sarah D. Brooks, German Vidaurre, and Daniel C. O. Thornton. 2014. “Using Raman Microspectroscopy to Determine Chemical Composition and Mixing State of Airborne Marine Aerosols over the Pacific Ocean.” *Aerosol Science and Technology* 48 (2): 193–206. <https://doi.org/10.1080/02786826.2013.867297>.
- Erickson, David J., and Robert A. Duce. 1988. “On the Global Flux of Atmospheric Sea Salt.” *Journal of Geophysical Research: Oceans* 93 (C11): 14079–88. <https://doi.org/10.1029/JC093iC11p14079>.
- Facchini, Maria Cristina, Matteo Rinaldi, Stefano Decesari, Claudio Carbone, Emanuela Finessi, Mihaela Mircea, Sandro Fuzzi, et al. 2008. “Primary Submicron Marine Aerosol Dominated by Insoluble Organic Colloids and Aggregates.” *Geophysical Research Letters* 35 (17). <https://doi.org/10.1029/2008GL034210>.
- Feingold, G., W. R. Cotton, S. M. Kreidenweis, and J. T. Davis. 1999. “The Impact of Giant Cloud Condensation Nuclei on Drizzle Formation in Stratocumulus: Implications for Cloud Radiative Properties.” *Journal of the Atmospheric Sciences* 56 (24): 4100–4117. [https://doi.org/10.1175/1520-0469\(1999\)056<4100:TIOGCC>2.0.CO;2](https://doi.org/10.1175/1520-0469(1999)056<4100:TIOGCC>2.0.CO;2).
- Flombaum, Pedro, José L. Gallegos, Rodolfo A. Gordillo, José Rincón, Lina L. Zabala, Nianzhi Jiao, David M. Karl, et al. 2013. “Present and Future Global Distributions of the Marine Cyanobacteria *Prochlorococcus* and *Synechococcus*.” *Proceedings of the National Academy of Sciences* 110 (24): 9824–29. <https://doi.org/10.1073/pnas.1307701110>.
- Galgani, Luisa, Christian Stolle, Sonja Endres, Kai G. Schulz, and Anja Engel. 2014. “Effects of Ocean Acidification on the Biogenic Composition of the Sea-surface Microlayer: Results from a Mesocosm Study.” *Journal of Geophysical Research: Oceans* 119 (11): 7911–24. <https://doi.org/10.1002/2014JC010188>.
- Garimella, Sarvesh, Thomas Bjerring Kristensen, Karolina Ignatius, Andre Welti, Jens Voigtlaender, Gourihar R. Kulkarni, Frank Sagan, et al. 2016. “The SPectrometer for Ice Nuclei (SPIN): An Instrument to Investigate Ice Nucleation.” *Atmospheric Measurement Techniques* 9 (7): 2781–95. <https://doi.org/10.5194/amt-9-2781-2016>.
- Garimella, Sarvesh, Daniel A. Rothenberg, Martin J. Wolf, Robert O. David, Zamin A. Kanji, Chien Wang, Michael Rosch, and Daniel J. Cziczo. 2017. “Uncertainty in Counting Ice Nucleating Particles with Continuous Flow Diffusion Chambers.” *Atmospheric Chemistry and Physics* 17 (17): 10855–64. <https://doi.org/10.5194/acp-17-10855-2017>.

- Graether, Steffen P., and Zongchao Jia. 2001. "Modeling *Pseudomonas Syringae* Ice-Nucleation Protein as A-Helical Protein." *Biophysical Journal* 80 (3): 1169–73. [https://doi.org/10.1016/S0006-3495\(01\)76093-6](https://doi.org/10.1016/S0006-3495(01)76093-6).
- Haywood, J., and O. Boucher. 2000. "Estimates of the Direct and Indirect Radiative Forcing Due to Tropospheric Aerosols: A Review." *Reviews of Geophysics* 38 (4): 513–43. <https://doi.org/10.1029/1999RG000078>.
- Hoose, C., and O. Möhler. 2012. "Heterogeneous Ice Nucleation on Atmospheric Aerosols: A Review of Results from Laboratory Experiments." *Atmos. Chem. Phys.* 12 (20): 9817–54. <https://doi.org/10.5194/acp-12-9817-2012>.
- IPCC, 2014: Climate Change 2014: Synthesis Report. Contribution of Working Groups I, II and III to the Fifth Assessment Report of the Intergovernmental Panel on Climate Change [Core Writing Team, R.K. Pachauri and L.A. Meyer (eds.)]. IPCC, Geneva, Switzerland, 151 pp.
- Junge, K., and B. D. Swanson. 2008. "High-Resolution Ice Nucleation Spectra of Sea-Ice Bacteria: Implications for Cloud Formation and Life in Frozen Environments." *Biogeosciences* 5 (3): 865–73. <https://doi.org/10.5194/bg-5-865-2008>.
- Ke, Wei-Ren, Yu-Mei Kuo, Chih-Wei Lin, Sheng-Hsiu Huang, and Chih-Chieh Chen. 2017. "Characterization of Aerosol Emissions from Single Bubble Bursting." *Journal of Aerosol Science* 109 (July): 1–12. <https://doi.org/10.1016/j.jaerosci.2017.03.006>.
- Kong, Xiangrui, Martin J. Wolf, Michael Roesch, Erik S. Thomson, Thorsten Bartels-Rausch, Peter A. Alpert, Markus Ammann, Nønne L. Prisle, and Daniel J. Cziczo. 2018. "A Continuous Flow Diffusion Chamber Study of Sea Salt Particles Acting as Cloud Nuclei: Deliquescence and Ice Nucleation." *Tellus B: Chemical and Physical Meteorology* 70 (1): 1463806. <https://doi.org/10.1080/16000889.2018.1463806>.
- Ladino, L. A., J. D. Yakobi-Hancock, W. P. Kalthau, R. H. Mason, M. Si, J. Li, L. A. Miller, et al. 2016. "Addressing the Ice Nucleating Abilities of Marine Aerosol: A Combination of Deposition Mode Laboratory and Field Measurements." *Atmospheric Environment* 132 (May): 1–10. <https://doi.org/10.1016/j.atmosenv.2016.02.028>.
- Lesins Glen, Petr Chylek, and Ulrike Lohmann. 2002. "A Study of Internal and External Mixing Scenarios and Its Effect on Aerosol Optical Properties and Direct Radiative Forcing." *Journal of Geophysical Research: Atmospheres* 107 (D10): AAC 5-1. <https://doi.org/10.1029/2001JD000973>.
- Lewis, E. R., W.J. Wiscombe, B. A. Albrecht; C. N. Flagg; R. M. Reynolds; A. P. Siebesma. 2012. "MAGIC: Marine ARM GPCI Investigation of Clouds." DOE/SC-ARM-12-020, U.S. Department of Energy, 12 pp.
- Moore Lisa R., Coe Allison, Erik R. Zinser, Mak A. Saito, Matthew B. Sullivan, Debbie Lindell, Katya Frois-Moniz, John Waterbury, and Sallie W. Chisholm. 2007. "Culturing the Marine Cyanobacterium *Prochlorococcus*." *Limnology and Oceanography: Methods* 5 (10): 353–62. <https://doi.org/10.4319/lom.2007.5.353>.
- Pandey, Ravindra, Kota Usui, Ruth A. Livingstone, Sean A. Fischer, Jim Pfaendtner, Ellen H. G.

- Backus, Yuki Nagata, et al. 2016. "Ice-Nucleating Bacteria Control the Order and Dynamics of Interfacial Water." *Science Advances* 2 (4): e1501630. <https://doi.org/10.1126/sciadv.1501630>.
- Prather, Kimberly A., Timothy H. Bertram, Vicki H. Grassian, Grant B. Deane, M. Dale Stokes, Paul J. DeMott, Lihini I. Aluwihare, et al. 2013. "Bringing the Ocean into the Laboratory to Probe the Chemical Complexity of Sea Spray Aerosol." *Proceedings of the National Academy of Sciences* 110 (19): 7550–55. <https://doi.org/10.1073/pnas.1300262110>.
- Pruppacher, Hans R, and James D Klett. 2011. *Microphysics of Clouds and Precipitation*. Dordrecht; Heidelberg; London: Springer.
- Pummer, B. G., C. Budke, S. Augustin-Bauditz, D. Niedermeier, L. Felgitsch, C. J. Kampf, R. G. Huber, et al. 2015. "Ice Nucleation by Water-Soluble Macromolecules." *Atmos. Chem. Phys.* 15 (8): 4077–91. <https://doi.org/10.5194/acp-15-4077-2015>.
- Rogers, David C. 1988. "Development of a Continuous Flow Thermal Gradient Diffusion Chamber for Ice Nucleation Studies." *Atmospheric Research* 22 (2): 149–81. [https://doi.org/10.1016/0169-8095\(88\)90005-1](https://doi.org/10.1016/0169-8095(88)90005-1).
- Salter, M. E., E. Hamacher-Barth, C. Leck, J. Werner, C. M. Johnson, I. Riipinen, E. D. Nilsson, and P. Zieger. 2016. "Calcium Enrichment in Sea Spray Aerosol Particles." *Geophysical Research Letters* 43 (15): 8277–85. <https://doi.org/10.1002/2016GL070275>.
- Schill, Gregory P., and Margaret A. Tolbert. 2014. "Heterogeneous Ice Nucleation on Simulated Sea-Spray Aerosol Using Raman Microscopy." *The Journal of Physical Chemistry C* 118 (50): 29234–41. <https://doi.org/10.1021/jp505379j>.
- Seinfeld, John H., and Spyros N. Pandis. 2006. *Atmospheric Chemistry and Physics: From Air Pollution to Climate Change*. 2 edition. Hoboken, N.J: Wiley-Interscience.
- Stokes, M. D., G. B. Deane, K. Prather, T. H. Bertram, M. J. Ruppel, O. S. Ryder, J. M. Brady, and D. Zhao. 2013. "A Marine Aerosol Reference Tank System as a Breaking Wave Analogue for the Production of Foam and Sea-Spray Aerosols." *Atmos. Meas. Tech.* 6 (4): 1085–94. <https://doi.org/10.5194/amt-6-1085-2013>.
- Vali, G., P. J. DeMott, O. Moehler, and T. F. Whale. 2015. "Technical Note: A Proposal for Ice Nucleation Terminology." *Atmospheric Chemistry and Physics* 15 (18): 10263–70. <https://doi.org/10.5194/acp-15-10263-2015>.
- Vergara-Temprado, J., B. J. Murray, T. W. Wilson, D. O'Sullivan, J. Browse, K. J. Pringle, K. Ardon-Dryer, et al. 2017. "Contribution of Feldspar and Marine Organic Aerosols to Global Ice Nucleating Particle Concentrations." *Atmos. Chem. Phys.* 17 (5): 3637–58. <https://doi.org/10.5194/acp-17-3637-2017>.
- Vignati, E., M. C. Facchini, M. Rinaldi, C. Scannell, D. Ceburnis, J. Sciare, M. Kanakidou, S. Myriokefalitakis, F. Dentener, and C. D. O'Dowd. 2010. "Global Scale Emission and Distribution of Sea-Spray Aerosol: Sea-Salt and Organic Enrichment." *Atmospheric Environment* 44 (5): 670–77. <https://doi.org/10.1016/j.atmosenv.2009.11.013>.
- Wang, Xiaofei, Grant B. Deane, Kathryn A. Moore, Olivia S. Ryder, M. Dale Stokes, Charlotte M. Beall, Douglas B. Collins, et al. 2017. "The Role of Jet and Film Drops in Controlling

the Mixing State of Submicron Sea Spray Aerosol Particles.” Proceedings of the National Academy of Sciences 114 (27): 6978–83. <https://doi.org/10.1073/pnas.1702420114>.

Wang, Xiaofei, Camille M. Sultana, Jonathan Trueblood, Thomas C. J. Hill, Francesca Malfatti, Christopher Lee, Olga Laskina, et al. 2015. “Microbial Control of Sea Spray Aerosol Composition: A Tale of Two Blooms.” ACS Central Science 1 (3): 124–31. <https://doi.org/10.1021/acscentsci.5b00148>.

Wilson, Theodore W., Luis A. Ladino, Peter A. Alpert, Mark N. Breckels, Ian M. Brooks, Jo Browse, Susannah M. Burrows, et al. 2015. “A Marine Biogenic Source of Atmospheric Ice-Nucleating Particles.” Nature 525 (7568): 234. <https://doi.org/10.1038/nature14986>.

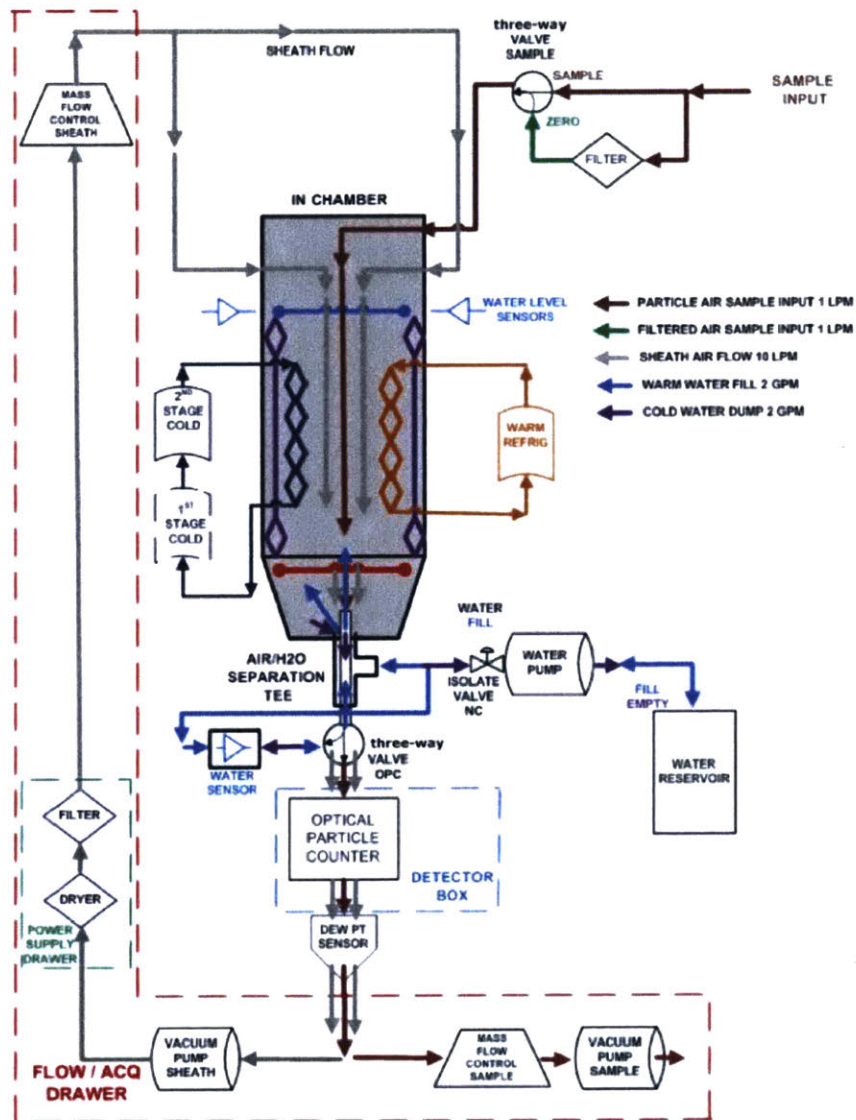
Wolf, Martin J., Allison Coe, Lilian A. Dove, Maria A. Zawadowicz, Keven Dooley, Steven J. Biller, Yue Zhang, Sallie W. Chisholm, Daniel J. Cziczo. "Investigating the Heterogeneous Ice Nucleation Potential of Sea Spray Aerosols Using *Prochlorococcus* as a Model Source of Marine Organic Matter." Submitted to Environmental Science and Technology.

Wurl, Oliver, Werner Ekau, William M. Landing, and Christopher J. Zappa. 2017. “Sea Surface Microlayer in a Changing Ocean – A Perspective.” Elem Sci Anth 5 (0). <https://doi.org/10.1525/elementa.228>.

Zhuang, Y., E.P. Lozowski, J.D. Wilson, and G. Bird. 1993. “Sea Spray Dispersion Over the Ocean Surface - a Numerical-Simulation.” Journal of Geophysical Research-Oceans 98 (C9): 16547–53. <https://doi.org/10.1029/93JC01406>.



# Appendix A



Air and water flow diagram of the SPIN chamber. Adapted from Garimella et al. (2016).

# Appendix B

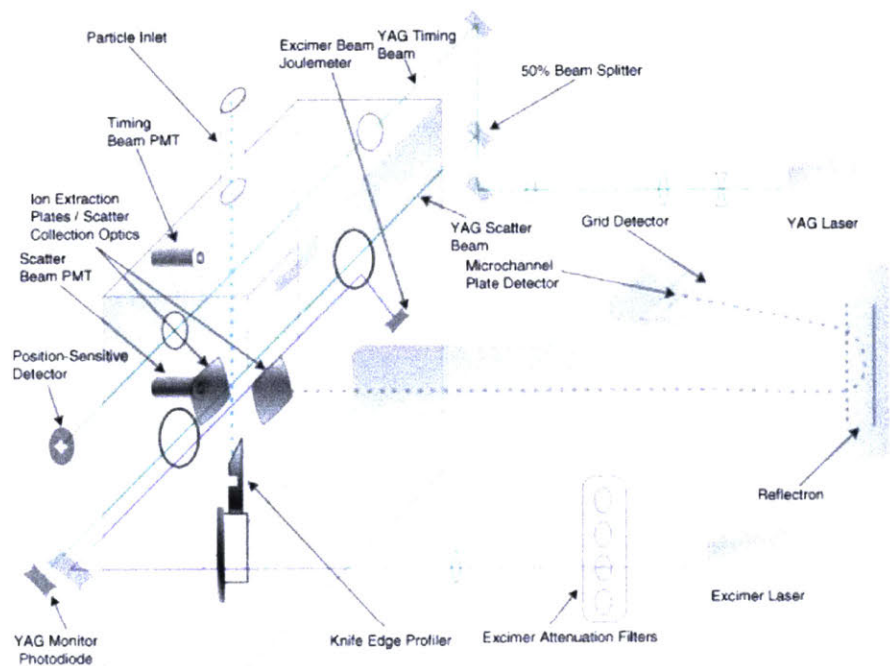


Diagram of the internal workings of the PALMS instrument. Adapted from Cziczo et al. (2006).